



# Investigation on Fabrication of Nanoscale Patterns Using Laser Interference Lithography

Jinnil Choi<sup>1</sup>, Myung-Ho Chung<sup>1</sup>, Ki-Young Dong<sup>1</sup>, Eun-Mi Park<sup>1</sup>, Dae-Jin Ham<sup>1</sup>, YunKwon Park<sup>2</sup>,  
In Sang Song<sup>2</sup>, James Jungho Pak<sup>3</sup>, and Byeong-Kwon Ju<sup>1,\*</sup>

<sup>1</sup>Display and Nanosystem Lab., College of Engineering, Korea University, Seoul 136-713, Korea

<sup>2</sup>Future IT Center Communication Lab., Samsung Advanced Institute of Technology, Yongin-si Gyeonggi-do, 446-712, Korea

<sup>3</sup>Department of Electrical Engineering, Korea University, Seoul 136-713, Korea

Nanoscale patterns are fabricated by laser interference lithography (LIL) using Lloyd's mirror interferometer. LIL provides a patterning technology with simple, quick process over a large area without the usage of a mask. Effects of various key parameters for LIL, with 257 nm wavelength laser, are investigated, such as the exposure dosage, the half angle of two incident beams at the intersection, and the power of the light source for generating one or two dimensional (line and dot) nanoscale structures. The uniform dot patterns over an area of 20 mm × 20 mm with the half pitch sizes of around 190, 250, and 370 nm are achieved and by increasing the beam power up to 0.600 mW/cm<sup>2</sup>, the exposure process time was reduced down to 12/12 sec for the positive photoresist DHK-BF424 (DongJin) over a bare silicon substrate. In addition, bottom anti-reflective coating (DUV-30J, Brewer Science) is applied to confirm improvements for line structures. The advantages and limitations of LIL are highlighted for generating nanoscale patterns.

**Keywords:** Laser Interference Lithography, Nanoscale Patterns, Nano-Fabrication.

## 1. INTRODUCTION

Fabrication of nanoscale structures have been considered by many researchers focusing on development of their potential applications in the microelectronics industry. These methods include nanoimprint lithography, electron beam lithography, focused ion beam patterning and scanning probe related technology.<sup>1</sup> However in order to account for a maskless, quick process over a large area and with simplicity of the apparatus, laser interference lithography (LIL) is a possible candidate for generating nanoscale structures. LIL is a well established concept where the basic principle is that an interference pattern between two coherent light waves are set up and recorded over a photosensitive layer to produce periodic structures. One-dimensional line pattern was generated from a single exposure and two successive exposures with 90° rotation of the sample in-between define a two-dimensional dot/column pattern.

Although LIL with utilization of various types of lasers with different wavelengths were reported previously, exploring the effects of several key parameters could provide further understanding especially for a relatively short

wavelength laser ( $\lambda = 257$  nm). By applying a 257 nm wavelength laser, higher resolution can be achieved<sup>2</sup> and faster exposure process becomes possible, with the availability of higher power value. Although improvements on size of structures and process time could be achieved by applying even shorter wavelength lasers, this could lead to poor temporal and spatial coherence.<sup>3</sup>

The main focus of this study is on the investigation of parameter effects for deep-ultraviolet LIL to fabricate single and double exposure patterns with the usage of a robust positive photoresist (DHK-BF424, high resolution and high etch resistance, DongJin), which was performed through various case studies. Also, bottom anti-reflective coating (BARC, DUV-30J, Brewer Science) was applied to explore its effects on one dimensional structures. Comparison will be drawn with the previously reported studies where appropriate.

## 2. EXPERIMENTAL DETAILS

A single beam Lloyd's mirror interferometer was applied for the experiments with Ar-Ion ( $\lambda = 257$  nm) laser used as the light source, see Figure 1(a). The laser with

\* Author to whom correspondence should be addressed.

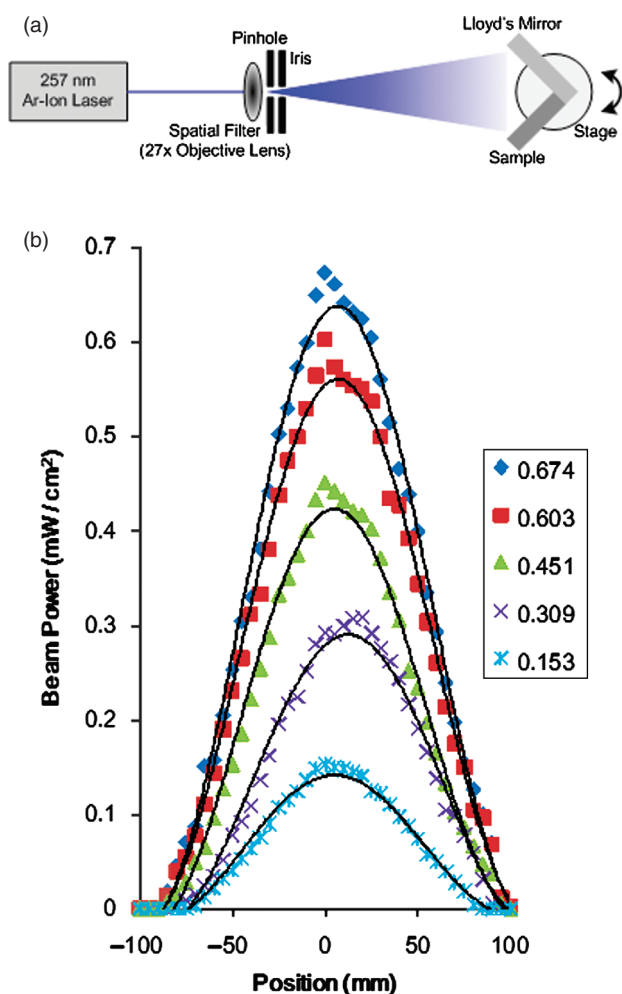


**Fig. 1.** (a) A schematic diagram of one beam LIL experimental apparatus and (b) Graphs of beam power against position of the detector with different maximum power.

515 nm wavelength was frequency doubled by a beta-barium borate (BBO) crystal, where the scheme was previously reported in Ref. [4]. Prior to the spin coating of the photoresist, a 3 cm × 3 cm Si substrate was cleaned with acetone, methanol, and deionized (DI) water, in that order. For better adhesion between the Si substrate and the photoresist, hexamethyldisilazane (HMDS) was spin coated for 30 sec at 2000 rpm on the bare silicon substrate, and then photoresist was spin coated for 25 sec at 4500 rpm, and baked at 110 °C for 60 sec. The final thickness of the photoresist measured by a surface profiler (Alpha-step, Dictak 3) was around 350 nm. The desired power was set by the optical power/energy meter (Newport, 1936-C) and with the sample loaded, the exposure was initiated. Then, the sample was post exposure baked (110 °C for 60 sec), which was followed by the development process with the according time conditions. Identical procedures were performed for numerous case studies, exploring the effects of the critical factors, namely, the exposure dosage, the

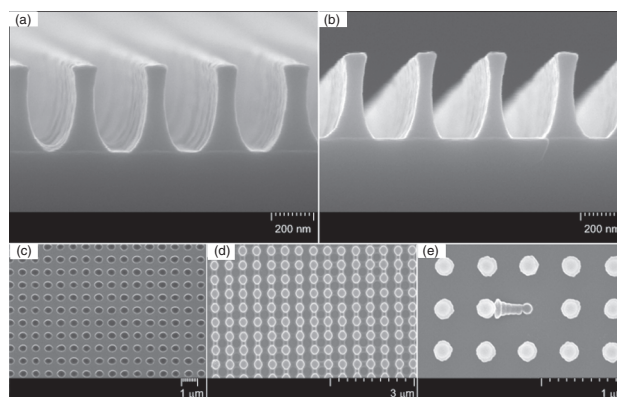


**Fig. 2.** SEM images of one dimensional (cross-sectional) and two dimensional patterns with variation of exposure dosages and develop time.

half angle between the two incident beams, and the beam power.

### 3. RESULTS AND DISCUSSION

Figure 2(a) shows the cross-sectional SEM images of line patterns with the aspect ratio of the columns of around 5:1 and the half pitch size of 150 nm.

In order to investigate the suitable exposure dosage for the current experimental conditions, case studies were performed with constant values of other parameters, such as LIL angle and beam power.

Figure 3 shows variation of doses for both single and dual exposures. Although some structures were not sufficiently developed, which could lead to non-uniform depth profiles, it can be clearly seen that a dosage of 13.5~15 mJ/cm<sup>2</sup> produced the best result for both types of patterns. Also SEM images were taken at random positions to confirm uniform patterns over the 20 mm × 20 mm area. Even with the utilization of a positive photoresist, insufficient dosage resulted in holes rather than columns (Fig. 2(c)), whereas excessive dosage could lead to inconsistent shape of patterns and collapse of the structure (Fig. 2(e)). These confirm the findings from references,<sup>5-7</sup>

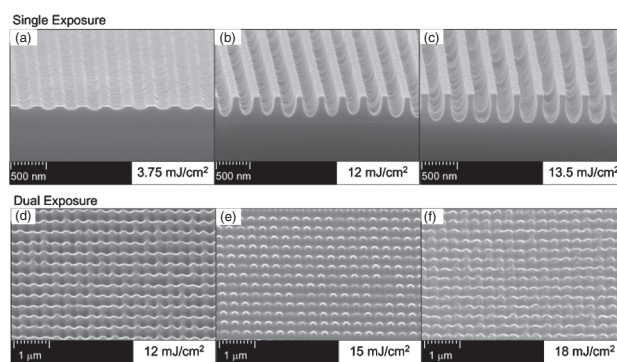


**Fig. 3.** SEM images of single and dual exposure with different exposure dosages (a) < (b) < (c) and (d) < (e) < (f).

where similar results have been reported. The gradual decrease in thickness of the nanoscale pillar seems to be due to the vertical standing waves caused by the reflection from the bare silicon substrate. Intensity distribution, energy distribution, is another crucial factor for generating periodic patterns over a sufficiently large area, where it is a function of the wave amplitude of the partial beams, the wavelength of the light source, and the LIL angle. Although the intensity distribution displayed changes, for a 20 mm × 20 mm area, seen in Figure 1(b), the distribution was sufficient enough to generate identical and periodical patterns.

With the required dosage defined, effects of the half angle between two beams at the intersection were explored by rotation of the stage. The relationship between the LIL angle ( $\lambda$ ) and the pitch of the pattern ( $\Lambda$ ) can be expressed as

$$\Lambda = \frac{\lambda}{2 \sin \theta} \quad (1)$$

By observing the size of the pitch and the LIL angle, it is apparent that Figure 4 agrees well with the above equation, itemized in Table I below, where the smallest size of the pitch is half the wavelength of the laser. However, in order to fabricate uniform patterns over an area of 20 mm × 20 mm, this theoretical value is unrealistic, especially due to the angle restriction in view of the geometry of the Lloyd's mirror interferometer.

As shown in Figure 4, two dimensional nanoscale structures were successively fabricated over an area of 20 mm × 20 mm for 10°, 15°, and 20° with pitches of around 741, 497, and 378 nm accordingly. For the one dimensional line patterns, uniform 310 nm sized pitches were achieved, see Figure 3(c). Although smaller pitches could be generated from shorter wavelength laser, which highlights the advantages of using 257 nm Ar-Ion laser, the experiments confirm the existing limitations in producing small, uniform patterns over a large area by LIL.

Finally, with a set exposure dosage, the power of the beam was varied in order to reduce the exposure time for quickening the LIL procedure. Although this process seems to be apparent, since the total energy applied to the

**Table I.** Comparisons between theoretical and actual pitch sizes of the fabricated patterns.

LIL Angle	Theoretical pitch size (nm)	Measured pitch size (nm)
10°	740	~741
15°	497	~497
20°	376	~378
25°	304	~310

sample is identical, the difficulties in realizing large area uniformity could be observed from the beam profile with different ranges of power (Fig. 1(b)). The actual area of exposure is around ±20 mm from the center (depending on the size of the sample), where it could be clearly seen that the power distribution varies more as the beam power is increased, which could cause inconsistent patterns. In this experiment, power was increased up to 0.600 mW/cm<sup>2</sup>, shortening the exposure process time to 12/12 sec, to produce similar results with patterns by application of lower power (0.150, 0.300, and 0.450 mW/cm<sup>2</sup>), see Figure 5. The dosage was set to be 13.5 mJ/cm<sup>2</sup> for all cases. Thus, this confirms the validity of the high power usage.

Additionally, experiments with the application of an anti-reflective coating were carried out for exploring its effects on one dimensional structures as shown in Figure 6.

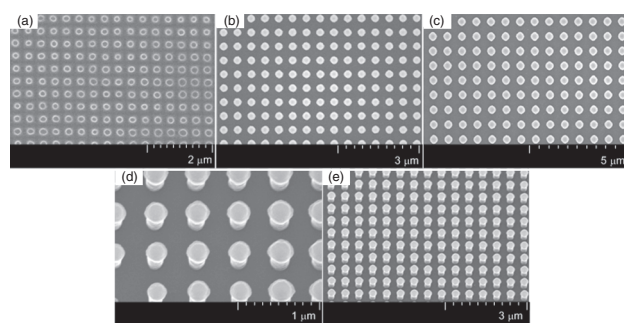


**Fig. 4.** (a)–(c) SEM images of two dimensional patterns with LIL angles of 20°, 15°, 10° respectively and (d)–(e) 45 degrees tilted SEM images with LIL angle of 15°.

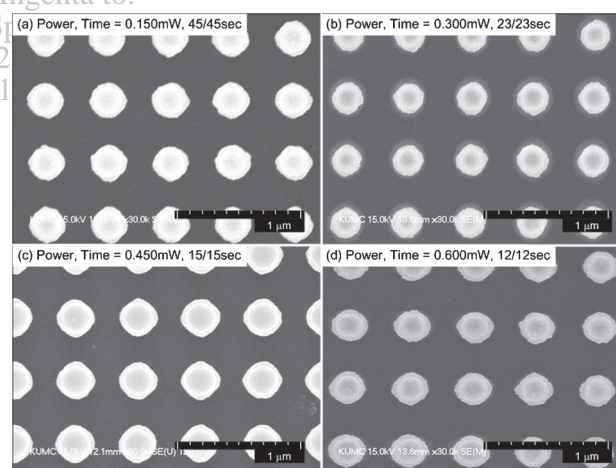


**Fig. 5.** SEM images of two dimensional patterns with different beam power (variation of exposure time).

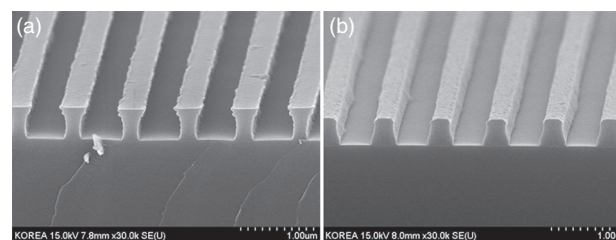


**Fig. 6.** SEM images of one dimensional patterns (a) with normal coating conditions and (b) with the application of BARC.

These comparison studies were performed under the same experimental conditions except for the application of bottom anti-reflective coating material (BARC). BARC was spin coated under the photoresist coating, to reduce the effects of the vertical standing wave. This was confirmed from observing Figure 6, where the decrease in thickness of the pillars were significantly smoothened.

#### 4. CONCLUSIONS

The effects of key factors in LIL have been investigated, such as the exposure dosage, the LIL angle, and especially the beam power for generating one and two dimensional nanoscale structures. From this study, the advantages and limitations of LIL are highlighted for generating nanoscale patterns. Among various patterning techniques, LIL is useful for its maskless, quick, and simple process characteristics, and improvements on LIL, such as quicker process, the capability of patterning over a large area,

and improving the patterns through application of anti-reflective materials could be advantageous.

**Acknowledgment:** This research was supported by Basic Science Research Program through the National Research Foundation of Korea (NRF) funded by the Ministry of Education, Science and Technology (No.2009-0083126).

#### References and Notes

1. A. D. Campo and E. Arzt, *Chem. Rev.* 108, 911 (2008).
2. S. R. J. Brueck, *Proceedings of the IEEE* 93, 10 (2005).
3. J. C. Lodder, *J. Magn. Magn. Mater.* 272–276, 1692 (2004).
4. W. Hinsberg, F. A. Houle, J. Hoffnagle, M. Sanchez, G. Wallraff, M. Morrison, and S. Frank, *J. Vac. Sci. Technol. B* 16, 3689 (1998).
5. A. Fernandez, J. Y. Decker, S. M. Herman, D. W. Phillion, D. W. Sweeney, and M. D. Perry, *J. Vac. Sci. Technol. B* 15, 2439 (1997).
6. Q. Xie, M. H. Hong, H. L. Tan, G. X. Chen, L. P. Shi, and T. C. Chong, *J. Alloy. Compd.* 449, 261 (2008).
7. R. Murillo, H. A. van Wolferen, L. Abelmann, and J. C. Lodder, *Microelectron. Eng.* 78, 260 (2005).

Received: 31 July 2009. Accepted: 28 December 2009.

Delivered by Ingenta to:  
Korea Institute for Special Education  
IP : 163.152.60.149  
Tue, 11 Jan 2011 16:33:53